

SUPPLEMENTAL MATERIAL

Expanded Materials and Methods

Data that support the findings of this study are available from the corresponding author upon reasonable request.

Cell lines, Quality Control, Culture, Differentiation and Treatment

The wild-type and BTHS iPSCs were described previously.¹⁰ The WT iPSCs are the PGP1 iPSCs line, modified with a doxycycline-inducible CRISPR/Cas9 transgene¹³. The BTHS iPSCs line, named BTHH, was generated from the WT line by Cas9-mediated introduction of a TAZ frameshift mutation reported in a BTHS patient. The Dox-induced Cas9 genome editing strategy (see below) was similarly used to introduce the TAZ mutation into an RYR2-S2814A (serine 2814 to alanine) mutant iPSC line (here designated WT-S2814A)¹⁴, yielding BTHH-S2814A. We previously sequenced top off-target candidate sites for RYR2 S2814A editing, and did not find mutations at these sites.¹⁴ To test for off-target mutations that may have been introduced during introduction of the TAZ frameshift mutation into the WT-S2814A cell line, we used CCTop-CRISPR/Cas9 target online predictor to search potential off-target sites (<https://cctop.cos.uni-heidelberg.de>). The top 10 candidate regions were PCR amplified from PGP1, BTHH, and BTHH-S2814A lines and subjected to Sanger sequencing (Table III in the Supplement). All iPSCs were cultured in mTesR medium (STEMCELL Technologies). Pluripotency of iPSCs was verified by immunostaining for pluripotency markers Oct4, Sox2, TRA-1-60 and SSEA4. Genome integrity was tested by digital karyotyping on the nanostring platform (Nanostring Technologies). Cell culture supernatants were routinely screened for mycoplasma contamination using PCR primers listed in Table I in the Supplement.

Monolayer cardiomyocyte differentiation was induced as previously described,^{15,16} with some minor modifications (Fig. I-A in the Supplement). Briefly, cells were detached by 3-5 min incubation with Versene (Invitrogen) and seeded onto 12-well plates pretreated with 1:1000 (v/v) diluted Geltrex (Life Technologies) at a density of 10,000 cells/cm². When cell confluency reached about 70%, cells were treated with basic medium (RPMI-1640 with 2 mM L-glutamine plus 1x B27 minus insulin) containing 6 μM CHIR99021 (STEMCELL Technologies) for 48 h, followed by basic medium containing 5 μM IWR-1-endo (STEMCELL Technologies) for another 48 h. After 6 more days in basic medium, cardiomyocytes were enriched by culture in lactate-containing media for 3 days⁴⁷ and then recovered for at least 3 days in RPMI-1640 with 2 mM L-glutamine plus 1x B27 with insulin. Unless otherwise indicated, iPSC-CMs were used between days 20-25 of differentiation.

For dissociation and re-plating, iPSC-CMs were treated with 1x accutase dissociation buffer (STEMCELL Technologies) for 10-15 min at 37°C. After removal of the buffer, cells were resuspended in culture medium supplemented with 5 μM RHO/ROCK inhibitor Y-27632, evenly seeded onto plates pre-coated with geltrex, and cultured overnight⁴⁸. The culture medium was replaced the following day with media without Y-27632. Re-plated CMs were cultured for at least 3 days prior to experimental analysis.

For modRNA transfection, TAZ expressing modRNA was synthesized and then introduced into iPSC-CMs as described previously¹⁰. For MitoTEMPO treatment, 5 μM MitoTEMPO was added to culture media daily for 3 days. For CaMKII inhibition, myristoylated autocamtide-2-related inhibitory peptide (AIP; final concentration 2.5 μM; Sigma-Aldrich) was added to culture medium daily for 24 h.

iPSC-CM Phenotypic Characterization

iPSC-CMs purity was measured by treating dissociated iPSC-CMs with Permeabilization/Fixation Buffer (BD Bioscience) for 20 min at room temperature, then incubated with 1:10 diluted APC conjugated anti-cTNT mouse antibody (Miltenyi Biotec) for 20

min at room temperature. Stained iPSC-CMs were analyzed using a BD FACS LSRFortesaa flow cytometer. Immunofluorescence microscopy for cTNT, ACTN2, MLC2A and MLC2V proteins were performed with primary antibodies shown in Table II in the Supplement.

Mitochondria were visualized by Mitotracker Green staining in live cells. Briefly, cells were seeded on 8 well μ -Slides (ibidi GmbH). After 5 days, cells were treated with 25 nM Mitotracker Green for 15 min and then washed 3 times prior to confocal imaging.

For cardiolipin analysis, lipids were extracted from iPSC-CMs and subjected to mass spectrometry as described previously.^{49,50}

iPSC-CM mitochondrial function was evaluated using the Agilent mitochondrial stress test. Briefly, WT or BTHH iPSC-CMs were isolated and seeded on a geltrex pre-coated 96-well Seahorse assay plate at 4×10^4 per well and cultured in RPMI+B27 medium for 3 days. Oxygen consumption rate (OCR) was measured using a Seahorse Biosciences XF96 extracellular flux analyzer and normalized to cell number, measured using the CyQUANT Cell Proliferation Assay Kit (Thermo Scientific). OCR was expressed as pmol/min/ 10^3 counts.

Genome Editing

For genome editing, we used iPSCs harboring a dox-induced Cas9 transgene^{13,14}. In order to introduce TAZ mutation into RYR2-S2814A iPSCs¹⁴, cells were treated with 2 μ M doxycycline overnight to induce Cas9 protein. The next day, cells were transfected with in vitro transcribed gRNAs (EnGen® sgRNA Synthesis Kit, NEB) plus DNA donor oligonucleotides (Life Technologies) using Human Stem Cell Nucleofactor Kit (Lonza #VPH-5012, program B-016). Three days after transfection, cells were dissociated and re-plated onto 10 cm dishes in a single cell format. Single cell-derived colonies were transferred to 24-well plates. Clone genotype was determined by Sanger sequencing of genomic DNA. Sequences of primers, gRNAs, and homology directed repair templates used in this study are provided in Table I in the Supplement.

Ca²⁺ Imaging

For ratiometric Ca²⁺ imaging, iPSC-CMs were plated on geltrex pre-coated 8 mm diameter coverslips. Cells were loaded with 4 μ M Fura-2 AM, 0.04% Pluronic F-127 (Life Technologies) in Tyrode's solution (Sigma-Aldrich) at 15 min at room temperature followed by 20 min washout. Ca²⁺ transients were recorded under 1 Hz pacing using the IonOptix Myocyte Calcium and Contractility System. To assess sarcoplasmic reticulum (SR) Ca²⁺ content, Fura-2 loaded cells were paced at 1 Hz for 30s prior to addition of 10 mM caffeine. Ca²⁺ peak amplitude ("normalized peak height") was calculated as (peak-baseline)/baseline x100.

SR Ca²⁺ leak was measured as described previously¹⁷. Fluo-3 AM loaded cells were paced at 1 Hz in normal Tyrode's solution, then perfused with 1 mM tetracaine in the absence of extracellular calcium and sodium (0 mM Ca²⁺ and 0 mM Na⁺ solution containing 5 mM 4-aminopyridine, 0.1 mM BaCl₂, 10 mM EGTA, 10 mM glucose, 10 mM HEPES, 4 mM KCl, 140 mM LiCl₂, 1 mM MgCl₂, 2 mM probenecid). The SR Ca²⁺ leak was defined as the tetracaine-induced reduction of intracellular Ca²⁺ concentration.

To quantify Ca²⁺ spark frequency, cells were transfected with an adenovirus that expressed GCaMP6f-Junctin (GCaMP6f-J) nanosensor¹⁸ and then imaged 36 hours post-transfection by confocal line scanning while maintaining cells at room temperature without pacing. Ca²⁺ sparks were counted for each cell.

For higher throughput Ca²⁺ imaging, we used the Vala Biosciences Kinetic Image Cytometer (KIC). iPSC-CMs were firstly infected with GCaMP5 lenti-virus (Addgene #46027). Three days later, cells were dissociated and seeded on polystyrene 96 well plates (Greiner Bio-One). After an additional three days, cells were stained with 0.1 μ g/ml Hoechst 33342 (Life Technologies) for 10 min and then imaged by KIC with a 20x objective at 30 frames per second. Three fields were randomly selected per well and imaged as following protocol: 1 Hz pacing for 15 sec prior to recording, then 1 Hz pacing for 10 sec, during which spontaneous Ca²⁺ release

were quantified, and then 10 sec without pacing, to measure spontaneous Ca^{2+} release frequency again. The imaging raw data was analyzed using CyteSeer software with the measurement program 'Trimmed Cell on Cell mask Average Pixel Intensity Function of Time'.

ROS Detection

For cellular ROS detection, dissociated iPSC-CMs were incubated with 5 μM CellROX Green (Life Technologies) at 37°C for 15 min and then washed 3 times before analysis using a BD FACS LSRFortessa flow cytometer. For mitochondrial ROS detection, mitochondria isolated using the Mitochondrial Isolation Kit (Life Technologies) were treated with 5 μM MitoSOX (Life Technologies) at 37°C for 15 min, then washed 3 times and analyzed using a BD FACS LSRFortessa flow cytometer. Data were analyzed using FlowJo by measuring the mean fluorescence intensity of each sample.

Protein expression

Protein expression was detected using the WES capillary western system (ProteinSimple). Cell extracts were diluted to 0.3 $\mu\text{g}/\mu\text{l}$ for most protein tests. Primary antibodies and their optimal dilution are shown in Table I in the Supplement. HRP-conjugated secondary antibodies were from ProteinSimple. Molecular weight of selected bands, calculated by WES based on migration of molecular weight standards, is labeled in the figures.

Detection of Oxidized RYR2

Oxidation of Ryanodine receptor was detected by measuring free thiols content as previous studies described⁵¹⁻⁵³ with some modifications. Briefly, Myocytes were lysed for total protein extraction. Then 1 μg anti-RYR2 antibody (Life Technologies) was added to at least 200 μg iPSC-CMs or 80 μg adult TAZ KO mice ventricles myocytes protein extract and incubated at 4°C for 2 h. Then mBBR (Life Technologies) was added at concentration of 1 mM and incubated at 4°C for 1 h. The antibody/antigen complex was then pulled out of the samples by 10 μg Protein G Dynabeads. Then the isolated RYR2 protein were loaded on NuPAGE 3-8% Tris-Acetate Protein Gels (Life Technologies). The fluorescence emission intensity of the RyR2-bound mBBR was measured at 482 nm by exciting at 382 nm. After mBBR fluorescence imaging, the gels underwent silver staining (Life Technologies) to detect RYR2 amount. To validate the sensitivity of this method, a positive control was set: a sample was treated with 100 μM H_2O_2 for 1 h at 4°C prior to antibody treatment.

SERCA2a Tyrosine Nitration Detection

SERCA2a Tyrosine Nitration was measured as described³⁴ with minor modifications. Briefly, 1 μg anti-Nitro-Tyrosine antibody (Life Technologies) was incubated with 40 μg iPSC-CMs protein extract at 4°C for 2 h. The antibody/antigen complex was precipitated using 10 μg Protein G Dynabeads. SERCA2a was detected by WES capillary western blotting.

Contractility Measurement

EHTs were generated as described previously²⁰ with some minor modifications. Briefly, 1.0×10^6 iPSC-CMs were used to generate each EHT. Only cultures with at least 70% iPSC-CM purity were used. Cells were transduced with adenovirus Chr2-YFP one day prior to assembly of EHTs. For full length TAZ expression, TAZ or RFP (control) modRNA was transfected into iPSC-CMs 3 days prior to EHT assembly. 3 days after EHT preparation, modRNA Taz was transfected again to maintain TAZ expression. Because modRNA has a limited lifespan of a few days, we modified EHT culture conditions for modRNA experiments to advance the time at which they developed contractile behavior. We modified the standard EHT culture medium (*EHT-medium* in the referenced literature²⁰) by replacing DMEM with RPMI 1640 plus B27 minus insulin, removing 10% heat-inactivated horse serum, and reducing aprotinin

concentration to 5 $\mu\text{g/ml}$. This resulted in EHTs initiating contraction as early as day 2-3 after EHT assembly, versus day 7-10 reported in the literature²⁰. EHTs treated with modRNAs were used for experiments on day 7 after EHT assembly. For other treatments, EHT contraction was recorded at 14 days after EHTs started contracting. For MT or AIP evaluation, EHT contraction was recorded before addition of these agents. Then the same EHTs were treated with AIP or MT for 1 day or 2 days, respectively, prior to video recording of their contractile activity.

EHTs were recorded using a BZ-X All-in-One Fluorescence Microscope (Keyence Corporation) with a 2x objective at 30 frames per second during 1 Hz optical pacing at 37°C. Contraction videos were analyzed by MuscleMotion²¹. To detect if sarcomere structures are different between WT and BTHH EHTs, EHTs were cryosectioned and stained for ACTN2. Sections were imaged using an Olympus FV-3000 confocal and analyzed using AutoTT⁵⁴.

TAZ knockout cardiomyocytes

Animal experiments were performed following protocols approved by Boston Children's Hospital Animal Care and Use Care Committee. Mice harboring a floxed allele of *Taz* were described previously^{23,27}. Mice were maintained in a C57BL6/J background.

Neonatal cardiomyocytes were dissociated from P1 to P3 *Taz*^{fllox/Y} ventricles using the Neonatal Heart Dissociation Kit (Miltenyi Biotec) and purified with the Neonatal Cardiomyocyte Isolation Kit (Miltenyi Biotec). After culture for two days, cells were treated with either adenovirus expressing *LacZ* (Ad:LacZ; control) or Ad:Cre (*Taz* knockout)⁵⁵. Experiments were performed 2-3 days later.

Taz^{fllox/Y}; *Myh6-Cre* (*Taz*^{cko}) and *Taz*^{WT/Y}; *Myh6-Cre* (control) mice were used for adult cardiomyocyte isolation. *Myh6-Cre* (Jax #011038)⁵⁶ is a Cre transgene that inactivates floxed alleles in cardiomyocytes. Adult ventricular cardiomyocytes were isolated from P60 mice by retrograde collagenase perfusion as described²⁵. For contractility assays, dissociated CMs were seeded on laminin coated coverslips and cultured in MEM medium supplemented with 10% FBS and 10 mM BDM (2,3-Butanedione 2-monoxime) for 0.5 h. The cells were then washed for 20 min to remove FBS and BDM and then imaged under 1 Hz pacing using the IonOptix Myocyte Calcium and Contractility System. For Ca^{2+} transient measurements, the seeded cells were loaded with 4 μM Fura-2 AM in the presence of 0.04% Pluronic F-127 (Invitrogen) for 15 minutes at room temperature followed by 20 minute washout. Ca^{2+} imaging was performed using the IonOptix Myocyte Calcium and Contractility System.

Murine Electrophysiology Studies

Taz^{fllox/Y}; *Myh6-Cre* (*Taz*^{cko}) and *Taz*^{WT/Y}; *Myh6-Cre* (control) mice were anesthetized by administration of isoflurane (1-3%) by nose cone. Monitoring of adequate anesthesia by touch pinch and normal respiratory effort was performed throughout the procedure. After achieving an appropriate level of anesthesia, platinum needle electrodes were placed in the upper and lower extremities to record standard ECG leads I and II. After removal of hair from the neck and upper right neck region, cannulation of the right jugular vein with a 1.1 French octapolar catheter was performed via a vascular cut-down. Proper catheter placement was confirmed by observation of characteristic ventricular electrograms and ventricular pacing response. Programmed ventricular extrastimulus testing was performed by delivery of a steady rate train of 8 paced beats (S1 x 8) followed by an early extra-stimulus (S2) with progressively shorter S1-S2 intervals. Loss of myocardial capture with the extra stimulus defined the ventricular effective refractory period (VERP). The procedure was then repeated with two extrastimuli (S2 and S3). For each stimulus epoch the S1-S2 or S2-S3 intervals were decreased by 5 msec at a time. Induction of ventricular or atrial arrhythmias were defined by more than 3 beats and the total duration was quantified. If an arrhythmia was induced, the same stimulus protocol was repeated two additional times and only arrhythmias induced by at least two of the three trials were quantified. Following stimulation at baseline, programmed ventricular stimulation was repeated after

intraperitoneal injection of isoproterenol (4 mg/kg), then epinephrine (2 mg/kg) plus caffeine (120 mg/kg). All drugs were delivered by intraperitoneal injection.

Statistical Analysis

All results are displayed as mean \pm SD. Normally distributed data was analyzed with Welch's two-tailed *t*-test (two groups) or ANOVA with Dunnett's post hoc test (three or more groups). Otherwise, we used the Kruskal-Wallis test with Dunn's post hoc test or a permutation test. Values of $P < 0.05$ were considered significant. In Figures 3, 4, and 5, data were acquired concurrently but presented in separate figures for clarity. The same vehicle and TAZ modRNA groups were used across these figures. The statistical analysis was performed once with all groups to appropriately correct for multiple testing.

Statistics were performed using GraphPad Prism 8 or R.

Suppl. Table 1. Primers and sequences used in this study.

Name	Sequence	Description
Myco-F	CACCATCTGTCACTCTGTAAAC	PCR for Mycoplasmas testing
Myco-R	GGAGCAAACAGGATTAGATAC	PCR for Mycoplasmas testing
S2814-F	ACACTATGTTTGGAAATTTGTGCCA	PCR for sequencing mutation on RYR2 gene
S2814-R	TGCTTTCCTGCATATATTTGGCA	PCR for sequencing mutation on RYR2 gene
RYR2-S2814-gR NA sequence	CAAATGATCTAGGTTTCTGTGG	gRNA synthesis
RYR2-S2814A oligos	AGGTTTTTAATGAGGCACTGTTTTTTCACACAAATG ATCTAGGTTGCTGTGGACGCTGCCCATGGTTACAGT CCCCGGGCCATTGACATGA	homology directed repair template
TAZ-F	TAAGCTAACCTGTCACCCCA	PCR for sequencing mutation on TAZ gene
TAZ-R	AGAGCACAGAGGCGAGGCTT	PCR for sequencing mutation on TAZ gene
A-F	AAGGAGCTGACAGAGGAA	Off-target sequencing for RYR2
A-R	AGGCTACAGTTAGGGTGG	Off-target sequencing for RYR2
B-F	CTAACCCACCAGTTTCTT	Off-target sequencing for BRK1
B-R	TGGAGTTTAACATGCCTAC	Off-target sequencing for BRK1
C-F	CCACATCTGATGCCAACTT	Off-target sequencing for LINC00173
C-R	GACCGAGTATTCCCGACA	Off-target sequencing for LINC00173
D-F	AAAATTGGGCACTGATGG	Off-target sequencing for RP11-196O2.1
D-R	AACTGCATTGCGGAGACA	Off-target sequencing for RP11-196O2.1
E-F	TTGGGATGGCAAAGAGCA	Off-target sequencing for CTD-2072I24.1
E-R	CTGGGAGAACAAGAATATGGA	Off-target sequencing for CTD-2072I24.1
F-F	GCAAACAGGGTTGGGATG	Off-target sequencing for RP11-664I21.5
F-R	AGGAGGCACTGGAGGGTA	Off-target sequencing for RP11-664I21.5
G-F	TCAGTGCGAGTCTATGGC	Off-target sequencing for AMPH
G-R	AGACAGTGGTGACGGTTG	Off-target sequencing for AMPH
H-F	CAAGCAATCCTCCCACCC	Off-target sequencing for JAZF1
H-R	CAGCCAGCCTTTCCCAGA	Off-target sequencing for JAZF1
I-F	AGATGAGGAGACAGGGGTGG	Off-target testing for FLJ16779
I-R	GGGGTTTCAGGGGAGCAG	Off-target testing for FLJ16779
J-F	GAGTCTTTTCCTCGTTGT	Off-target testing for AC108056.1
J-R	GTTGTGCAGCTTGTGATA	Off-target testing for AC108056.1
mWT-F	CTTGCCCACTGCTCACAAAC	TAZ KO mouse genotyping
mWT-R	CAGGCACATGGTCCTGTTTC	TAZ KO mouse genotyping
mKO	CCAAGTTGCTAGCCCACAAG	TAZ KO mouse genotyping

Suppl. Table 2. Antibodies used in this study

Antibody	Source	Cat. No.	Application	Dilution
CaMKII	Abcam	ab134041	WES	1:200
Phospho-CaMKII (Thr286)	CST	12716S	WES	1:100
Oxidized CaMKII (Met/281/282)	Millipore	07-1387	WES	1:200
p-RYR2	Badrilla	A010-31AP	WES	1:50
GAPDH	Life Tech	PA116777	WES	1:400
Vinculin	Santa Cruz	SC-25336	WES	1:400
Tafazzin	Santa Cruz	SC-365810	WES	1:50
Phospholamban (pThr17)	Badrilla	A010-13	WES	1:1500
Phospholamban	CST	14562S	WES	1:250
cTNT-FITC	Miltenyi Biotec	130-119-57 5	IFA	1:100
cTNT-APC	Miltenyi Biotec	130-119-57 5	FACS	1:100
ACTN2	Abcam	ab68168	IFA	1:200
MLC2A	Abcam	ab68086	IFA	1:250
MLC2V	Abcam	ab79935	IFA	1:250
RYR2	Life Tech	C3-33	IP	1 µg to per 80 µg adult mice CMs or 200 µg iPSC-CMs protein extract
SERCA2	CST	9580	WES	1:100
Nitro-Tyrosine	CST	9691	IP	1 µg to per 40 µg protein extract

Suppl. Table 3. Targeted sequencing did not detect off-target Cas9 editing by the BTHH guide RNA. The TAZ-targeted and top 10 off-target sites predicted by CCTop (see methods) were PCR amplified and evaluated by Sanger sequencing. Off target sites are shown with mismatches to gRNA sequence shown in red. Mut indicates the HDR-targeted mutation in Taz. Check indicates the wild-type sequence.

Coordinates	Associated Gene	Sequence	WT	BTHH	BTHH-2814A
chrX:154419583-154419605	TAZ	GAAGCTCAACCATGGGGACT	√	Mut	Mut
chr1:237784936-237784958	RYR2	GCACCTCAGGCATGGGGACT	√	√	√
chr3:10127061-10127083	BRK1	AAAGTCCAAACATGGGGACT	√	√	√
chr12:116534198-116534220	LINC00173	GAAGGTCCCCACGGGGACT	√	√	√
chr7:36096500-36096522	RP11-19602.1	GTGGCACAGCCATGGGGACT	√	√	√
chr5:7924664-7924686	CTD-2072I24.1	CCAGCACAAAGCATGGGGACT	√	√	√
chr11:124882759-124882781	RP11-664I21.5	GAGGCAGGACCATGGGGACT	√	√	√
chr7:38606132-38606154	AMPH	AAACCTAAAGCATGGGGACT	√	√	√
chr7:27899919-27899941	JAZF1	GGAGCTGGAGCATGGGGACT	√	√	√
chr20:63262897-63262919	FLJ16779	GAGCCCAACCCTGGGGACT	√	√	√
chr4:117898307-117898329	AC108056.1	GAAGCCCCACCTTGGGGACT	√	√	√

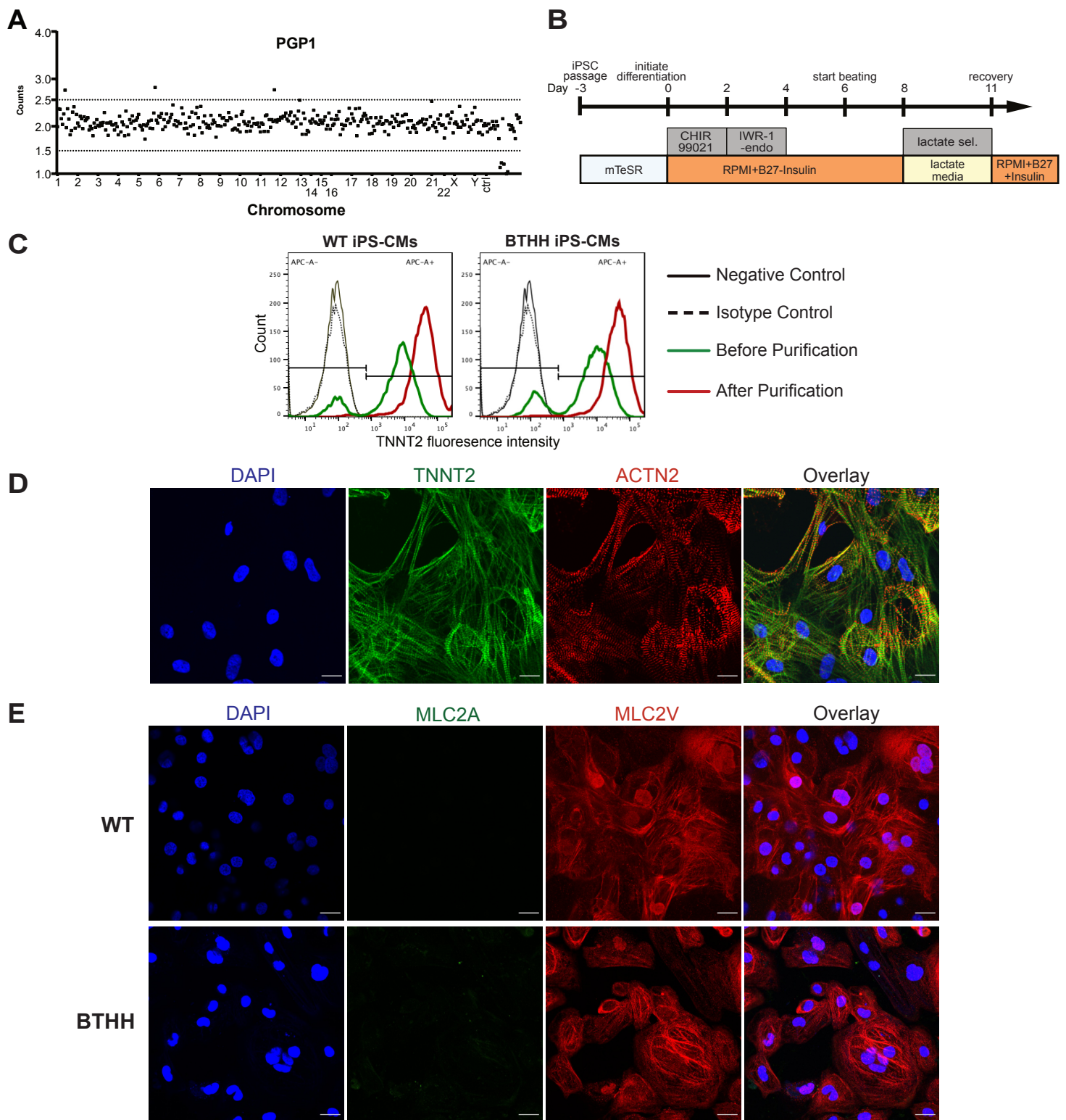


Fig. 1. Characterization of iPSC-CMs differentiated from PGP-1 iPSCs.

A. Nanostring human karyotyping assay on PGP1 iPSC cell line. Consecutive probes with values outside of the normal range (2 ± 0.5) were not observed. Individual probes slightly out of range are not predictive of copy number variation. **B.** Protocol to differentiate iPSCs to iPSCs-CMs. **C.** iPSC-CM purity. WT or BTHH iPSCs-CMs were stained for cardiac troponin T (TNNT2) and analyzed by flow cytometry. Purity was about 80% and >97% before and after lactate selection, respectively. **D.** Morphology of iPSCs-CMs. iPSC-CMs were stained for sarcomere proteins ACTN2 and TNNT2 and imaged with a confocal microscope. Scale bar = 10 μ m. **E.** Expression of ventricular and atrial marker genes. WT (upper) or BTHH (bottom) iPSCs-CMs staining with ventricle marker MLC2V and immature/atrial marker MLC2A showed that large majority of both cell lines expressed MLC2V but not MLC2A. Scale bar = 20 μ m.

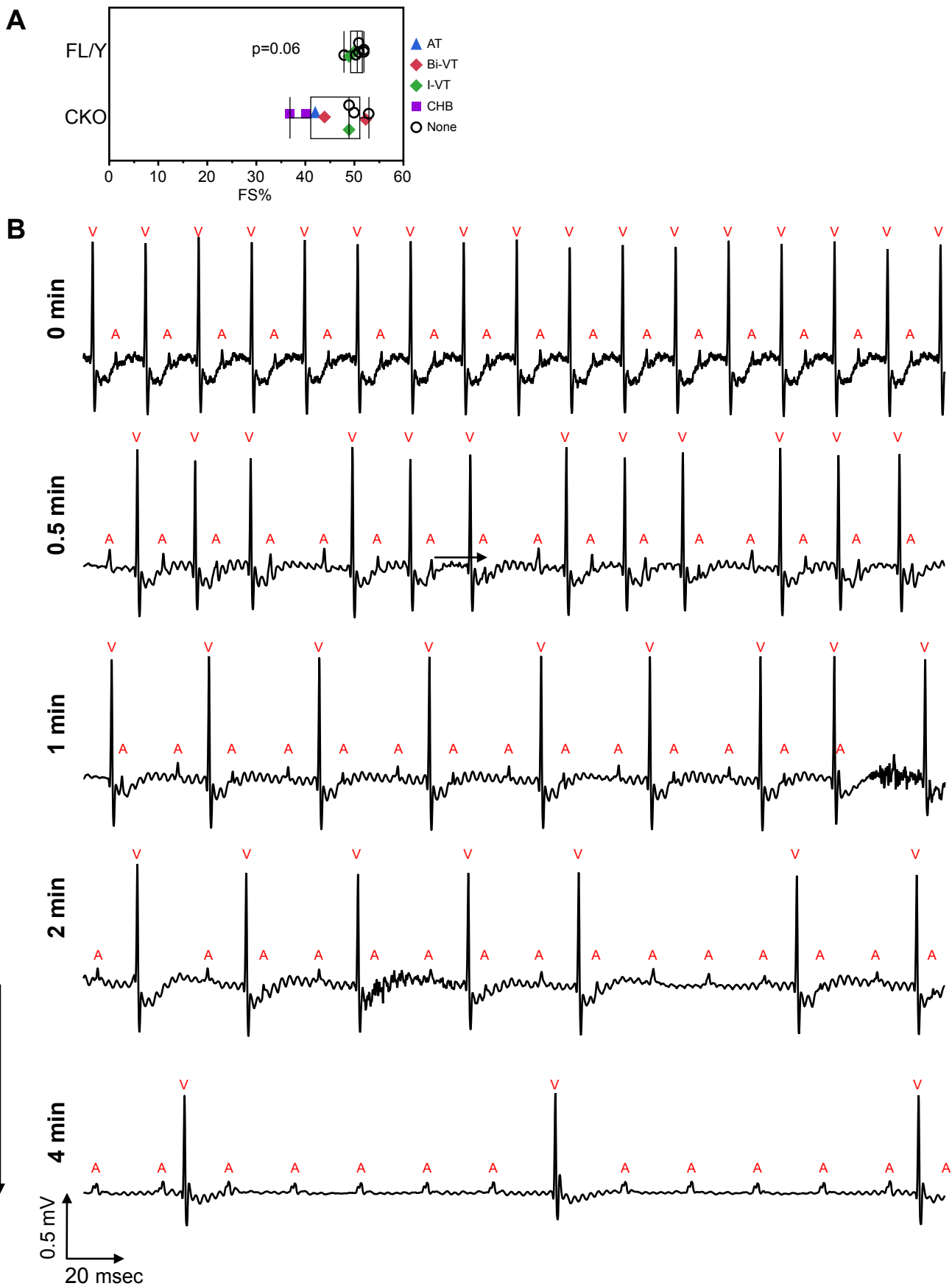


Fig. II. Progressive complete heart block in a TAZ CKO mouse. **A**. Systolic heart function of TAZ CKO and control mice. Heart function of CKO mice at the time of the EP study (6 weeks) was not significantly impaired. **B**. TAZ CKO mouse was anesthetized and surface electrocardiograms recorded at the indicated times after anesthesia induction with isoflurane delivered by nose cone and cannulation of the jugular vein. The mouse developed first degree AVB (1 min), Mobitz type I second degree AVB (0.5 min), and third degree AVB with a junctional escape rhythm (4 min). "A" and "V" mark atrial and ventricular depolarization, respectively.

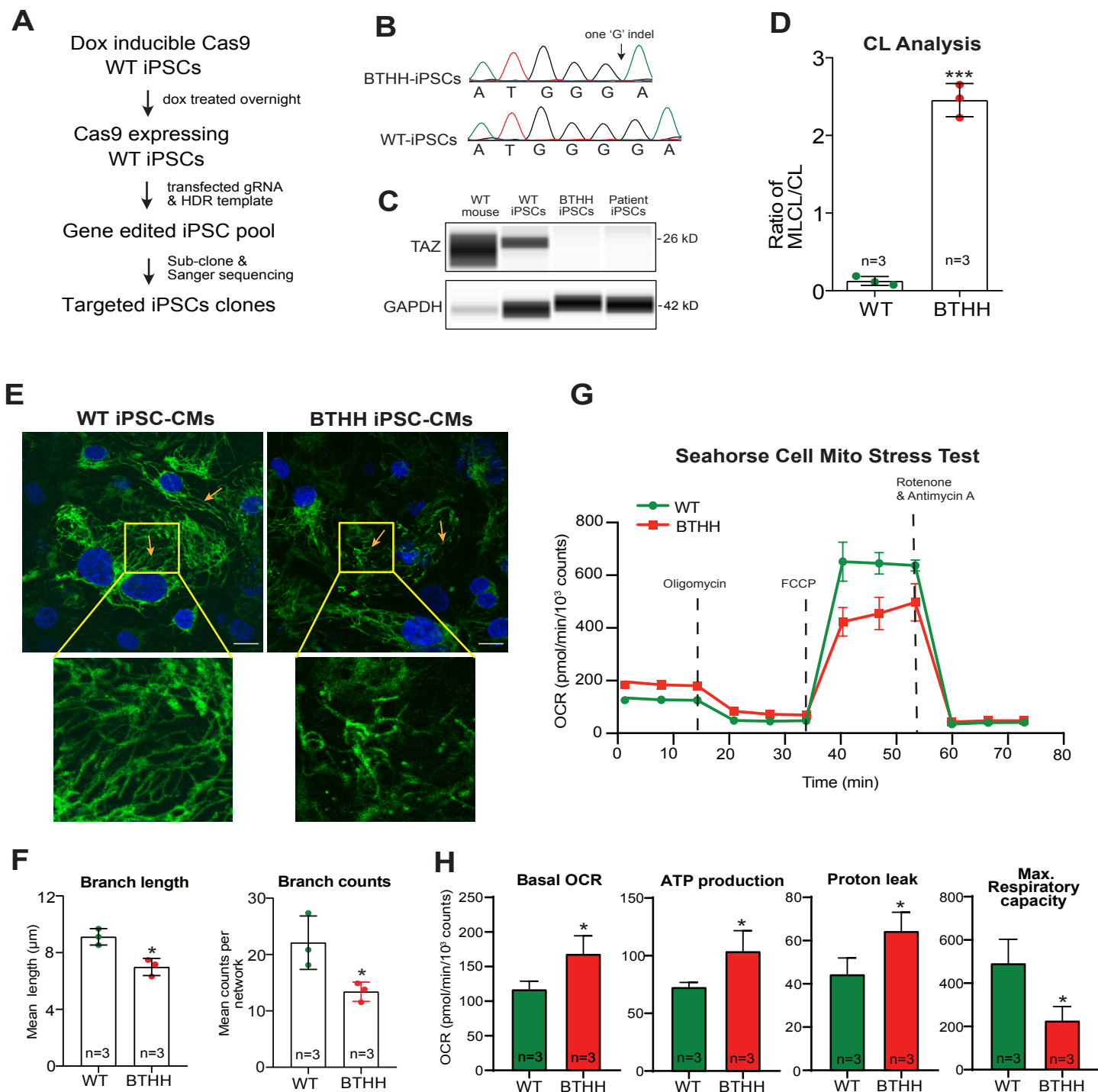


Fig. III. Characterization of BTHH and WT iPSC-CMs. **A.** Protocol for genome editing using Cas9 inducible iPSCs. **B.** The BTHH line was generated from PGP1 by using Cas9-mediated homology-directed repair to delete a 'G' residue in the *TAZ* gene. The mutation was verified by Sanger sequencing. **C.** Capillary western verified that TAZ protein was ablated in isogenic PGP1 *Taz* mutant iPSCs (BTHH) and BTHS patient iPSCs (pBTHH). Wild-type mouse ventricular cardiomyocytes and PGP1 iPSCs were used as positive controls. **D.** Abnormal cardiolipin profile of BTHH iPSC-CMs. Mass spectrometry demonstrated markedly elevated ratio of monolysocardiolipin (MLCL) to cardiolipin (CL). $n=3$. Two-tailed t -test: *** $P < 0.001$. **E-F.** Abnormal mitochondrial network morphology of BTHH iPSC-CMs. iPSC-CMs were stained with mitotracker green and imaged with a confocal microscope. **E.** Representative images. Boxed area is magnified in the lower images. Scale bar = $20 \mu\text{m}$. **F.** Quantitative analysis of mitochondrial network morphology. Two-tailed t -test. **G-H.** Abnormal mitochondrial function of BTHH iPSC-CMs. The Agilent mitochondrial function assay was performed on BTHH and control iPSC-CMs. **G.** Representative traces. Oxygen consumption rate (OCR) was normalized to viable cell counts. **H.** Statistical analysis of basal OCR, OCR attributable to ATP production, proton leak, and maximal respiratory capacity. $n=3$. Two-tailed t -test. * $P < 0.05$.

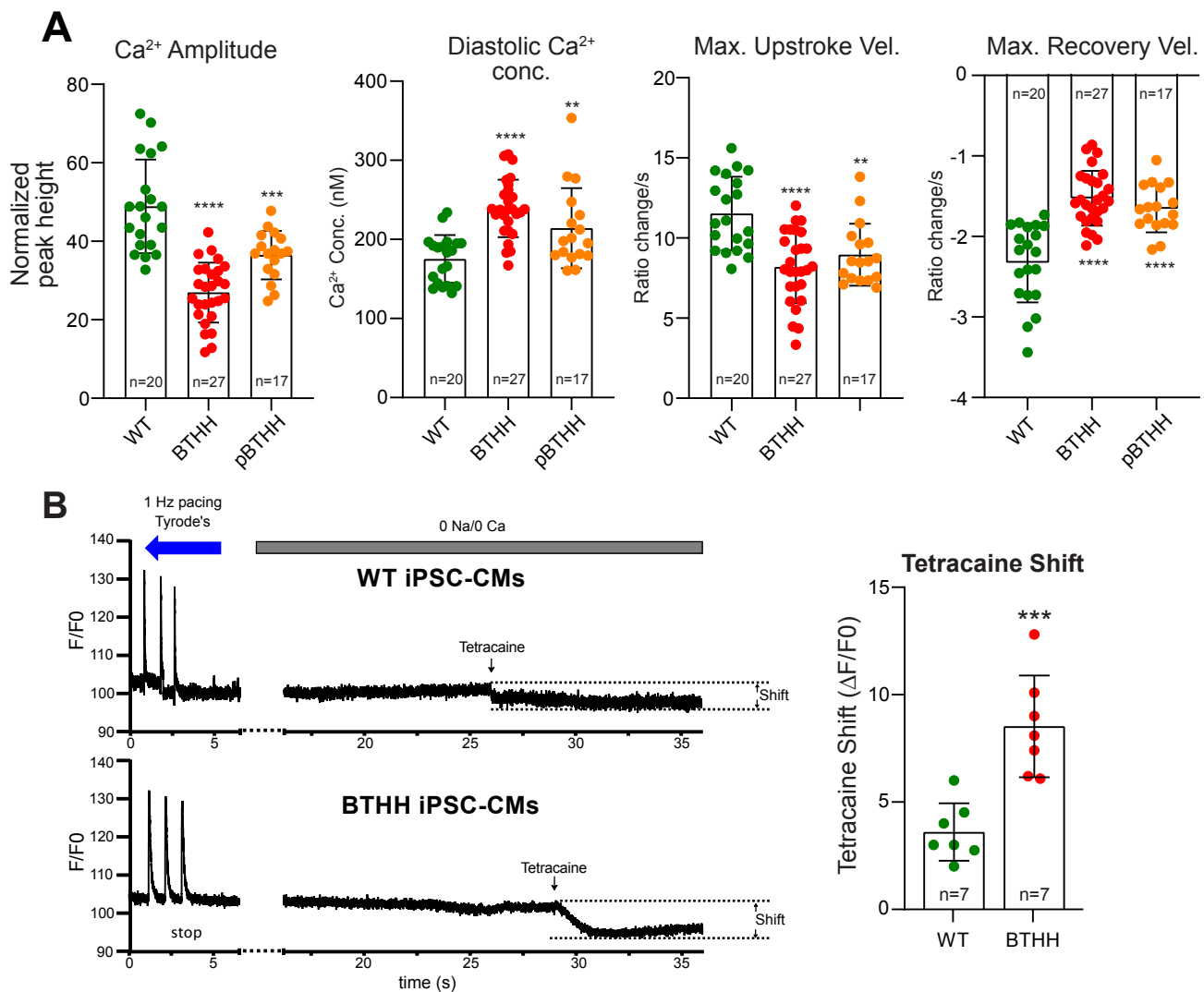


Fig. IV. Aberrant Ca^{2+} handling in BTHH iPSC-CMs. **A.** Quantitative analysis of the Ca^{2+} transient amplitude, diastolic Ca^{2+} concentration, maximal Ca^{2+} upstroke and recovery velocities of Barth syndrome patient iPSC-CMs (pBTHH) paced at 1 Hz. Each dot represents a different cell. **B.** The relative diastolic Ca^{2+} flux through RYR2 was measured using the "tetracaine shift" technique (see "Methods"). Left: representative "tetracaine shift" traces of WT and BTHH iPSC-CMs, respectively. Right: Quantitative analysis showed the tetracaine shift was significantly greater in BTHH iPSCs-CMs compared to WT. Two-tailed *t*-test, ** $P < 0.01$. *** $P < 0.001$. **** $P < 0.0001$ (continued on next page)

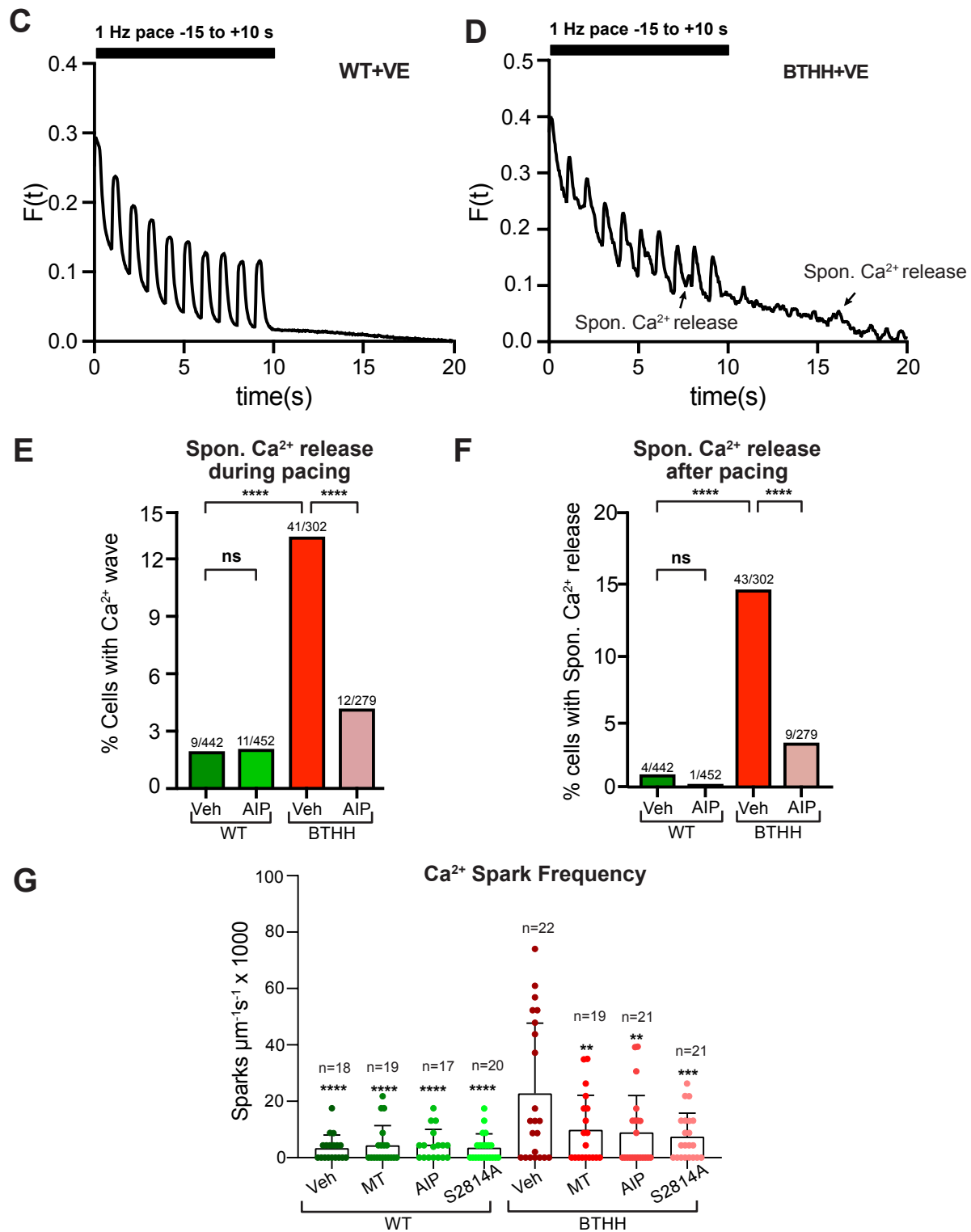


Fig. IV, continued. C-F. BTHH and WT iPSC-CMs were treated with GCaMP5 lenti-virus and paced electrically for 15 sec prior to imaging, imaged with continued pacing for 10 sec, and then imaged for an additional 10 sec without pacing. Irregularities of the Ca²⁺ transients during pacing and variation in baseline Ca²⁺ signal during the unpaced interval were defined as spontaneous Ca²⁺ release activity. C,D. Representative traces. E,F Quantitative analysis showed markedly higher frequency of spontaneous Ca²⁺ release in BTHH iPSCs-CMs compared to WT. AIP largely inhibited these abnormal Ca²⁺ release events. Chi-square test. **G.** Elevated Ca²⁺ spark frequency in BTHH iPSC-CMs was attenuated by ROS scavenging (MT), CaMKII inhibition (AIP), and ablation of RYR2-S2814A phosphosite. Ca²⁺ spark frequency was measured using confocal line scan imaging and the GCaMP6f-Junctin nanosensor. Elevated spark frequency in BTHH was ameliorated by MT, AIP, or RYR2-S2814A mutation. ANOVA with Dunnett's posthoc test, compared to BTHH+Veh. ** P<0.01. *** P<0.001. **** P<0.0001. ns, not significant.

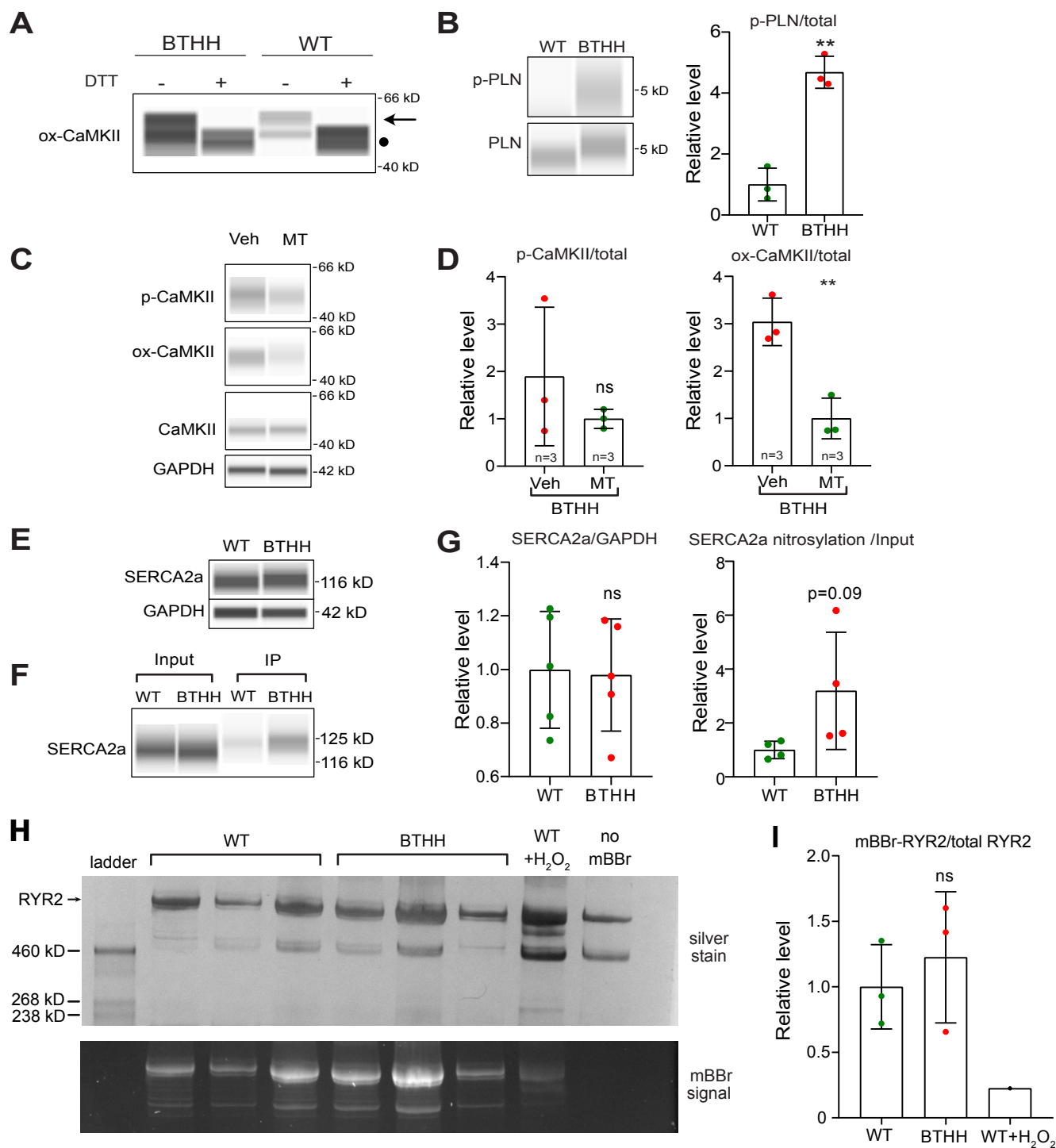


Fig. V. Post-translational modifications of CaMKII and SERCA2a in BTHH and WT iPSC-CMs. **A.** Specificity test of ox-CaMKII antibody. Protein extract was or was not treated with reducing agent dithiothreitol (DTT). Reducing agent decreased immunoreactivity of the ox-CaMKII band (arrow). Circle, non-specific band. **B.** Effect of TAZ mutation on CaMKII activity, as assessed by PLN-T17 phosphorylation (PLN monomer). Left, representative capillary western images. Right, quantitative analysis. **C-D.** Effect of MT on CaMKII activation in TAZ mutant and control iPSC-CMs. **C,** representative capillary western blot. **D,** quantitative analysis. **E-G.** SERCA2a nitrosylation detection. SERCA2A was immunoprecipitated using nitrotyrosine antibody and detected with SERCA2a antibody. Representative capillary western blots show total SERCA2a (**E**) and SERCA2a before and after nitrotyrosine IP (**F**). **G,** Quantitative analysis. **H-I.** RYR2 oxidation measured by monobromobimane (mBBr) assay. Immunoprecipitated RYR2 proteins were stained with mBBr, which fluoresces upon reaction with free thiols. **H,** Upper panel, silver stained gel. Lower panel, mBBr signal. Positive control H₂O₂-treated sample showed strongly reduced mBBr signal. Sample without mBBr treatment showed no fluorescent signal. The assay did not detect a significant change in RYR2 oxidation between genotypes. Two-tailed *t*-test. ** *P*<0.01. ns, *P*>0.05.

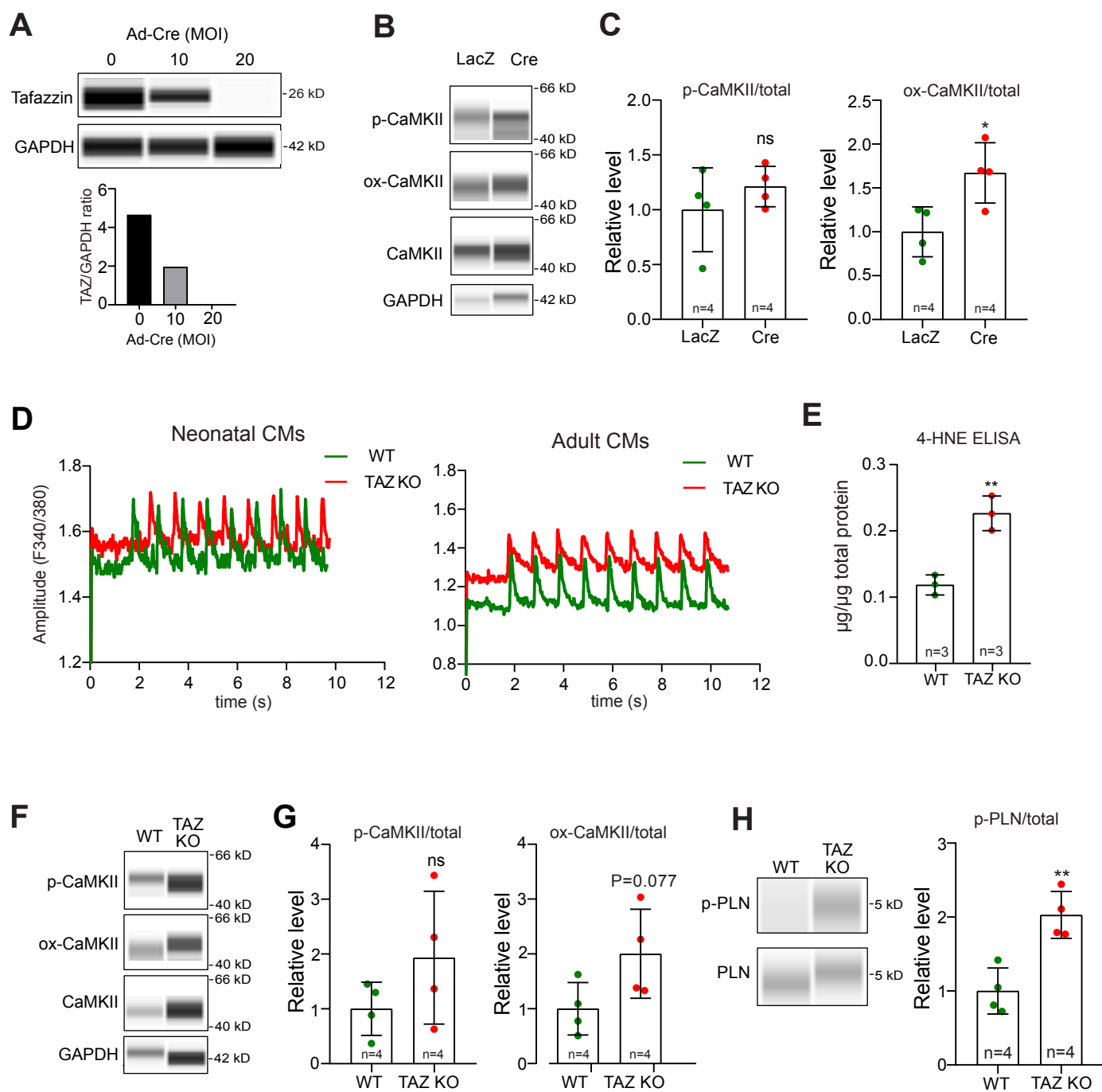


Fig. VI. Taz ablation in murine cardiomyocytes. **A.** TAZ knockout in cultured neonatal murine ventricular cardiomyocytes by adenovirus-mediated Cre expression. Ad-Cre was delivered at the indicated multiplicity of infection (MOI). The level of TAZ protein was measured by capillary western. **B-C.** Effect of Taz ablation on CaMKII post-translational modifications in neonatal murine ventricular cardiomyocytes. **B,** representative capillary western images. **C,** quantitative analysis. **D.** Representative Ca^{2+} transients of neonatal or adult WT and TAZ KO CMs imaged by Fura-2. Cells were electrically paced at 1 Hz. **E.** Effect of Taz ablation on lipid peroxidation product 4-HNE in adult heart ventricles. 4-HNE was measured by ELISA. Two-tailed *t*-test. **F-G.** Effect of Taz ablation on CaMKII post-translational modifications in adult murine ventricular cardiomyocytes. **F,** representative capillary western images. **G,** quantitative analysis. Two-tailed *t*-test. **H.** Capillary western showed significantly higher phosphorylated phospholamban (PLN-pThr17) level, normalized to total PLN, in TAZ KO adult mouse ventricle compared to WT. Left, representative capillary western plots. Right, quantification. Two-tailed *t*-test. ns, $P > 0.05$; * $P < 0.05$; ** $P < 0.01$.

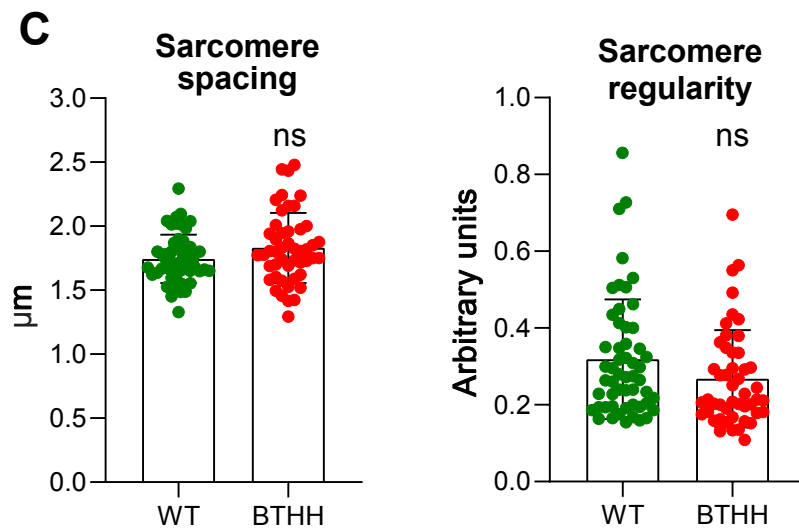
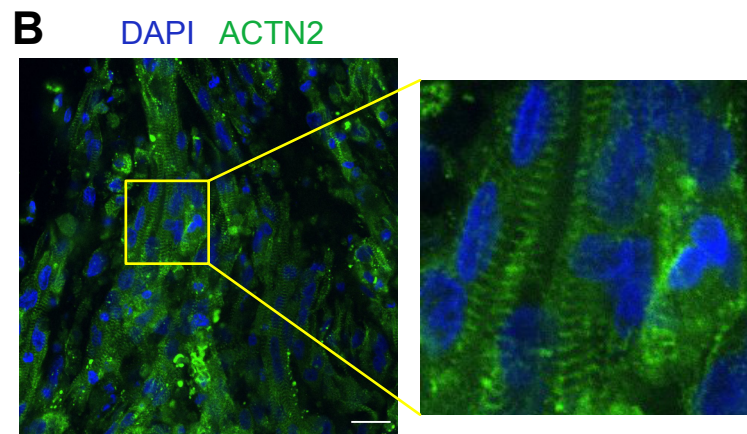
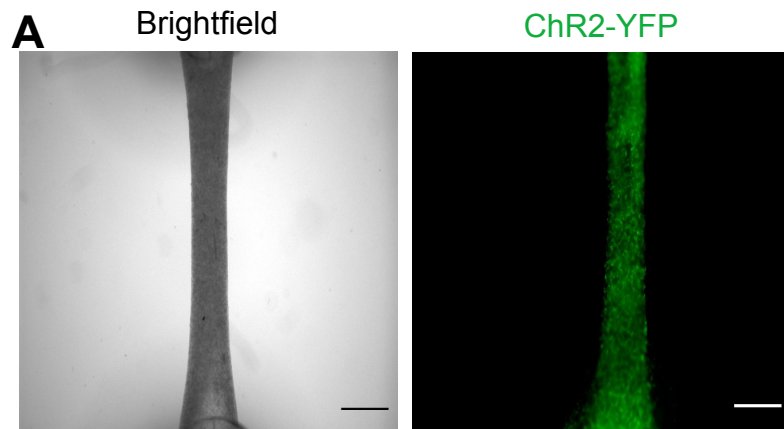


Fig. VII. EHTs assembled from iPSC-CMs. A. Brightfield and epifluorescent images of ChR2-YFP expressing EHT. bar = 1 mm. **B.** Immunofluorescent staining of EHT after one month of spontaneous contraction demonstrating well aligned sarcomeres. Boxed area is magnified to right. bar = 20 µm. **C.** AutoTT analysis showed no significant difference in sarcomere spacing and regularity between WT and BTHH EHTs. Two-tailed *t*-test.

Supplemental Video Legends

Supplemental Video 1. Imaging of iPSC-CM contraction and Ca²⁺ transients. A.

Representative video showing contraction of PGP1 iPSC-CMs in a monolayer. Metabolically selected iPSCs-CMs were dissociated and re-plated onto 12 wells plates. Scale bar = 100 μ m.

B. Representative video of PGP1-iPSCs-CMs infected with lenti-GCaMP5. Cells were imaged using the Vala Biosciences Kinetic Imaging Cytometer at 30 frames per second at 37°C with 1 Hz electrical pacing. Scale bar = 100 μ m.

Supplemental Video 2. Contraction of WT and BTHH EHTs. Videos were recorded 14 days after the start of visible EHT contraction. EHTs were optically paced at 1 Hz and recorded at 37°C. Scale bar = 1 mm.

Supplemental Video 3. Contraction of WT and BTHH EHTs after treatment with TAZ or RFP modified mRNA. Time course of experiment is shown in Fig. 7B. All EHTs were optically paced at 1 Hz and recorded at 37°C. Scale bar = 1 mm.

Supplemental Video 4. Contraction of WT and BTHH EHTs before and after treatment with MT. Time course of experiment is shown in Fig. 7B. All EHTs were optically paced at 1 Hz and recorded at 37°C. Scale bar = 1 mm.

Supplemental Video 5. Contraction of WT and BTHH EHTs before and after treatment with AIP. Time course of experiment is shown in Fig. 7B. All EHTs were optically paced at 1 Hz and recorded at 37°C. Scale bar = 1 mm.